UCRL-ID-129921

The Status Report of the Single Heater Test Chapter 4 Integrated Analyses

Wunan Lin

February 26, 1998

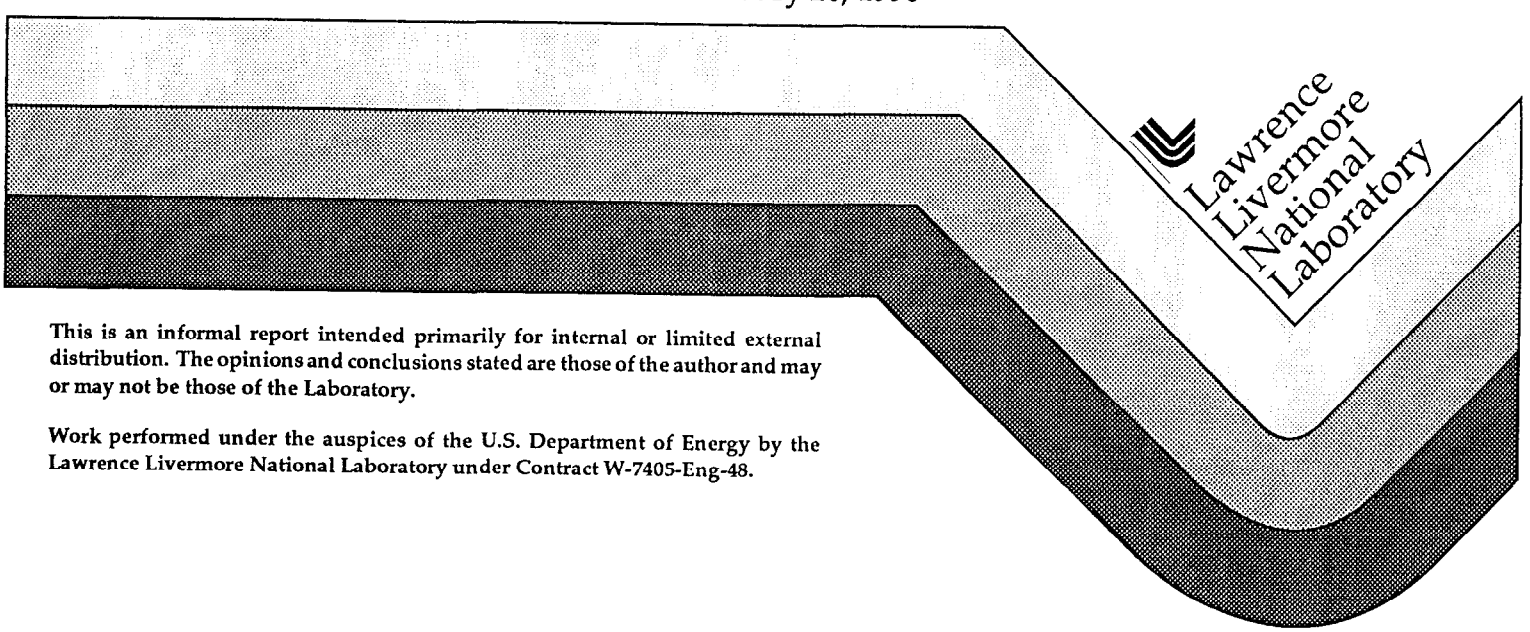

Work performed under the auspices of the U.S. Department of Energy by the Lawrence Livermore National Laboratory under Contract W-7405-Eng-48.

The Status Report of the Single Heater Test
Chapter 4 Integrated Analyses

Milestone #SP9266M4

Wunan Lin

4.3 Hydrological Responses

The primary purposes of the Single Heater Test (SHT) are to study the thermal-mechanical responses of the heated block. The SHT is too small and does not have adequate access for a complete study of the coupled thermal-mechanical-hydrological-chemical processes. The SHT is used as a shake-down/scoping study for the thermal-hydrological-chemical processes. For the thermal-hydrological process, the temporal and spatial variations of the moisture content in the heated block are monitored by neutron logging in Holes 15, 17, 22, and 23, electrical resistivity tomograph (ERT) in Holes 24 to 27. In addition, relative humidity, gas pressure, and temperature are measured in zones between packers in Holes 16 and 18. Temperature is also measured by resistance temperature devices (RTD) in the neutron logging holes (15, 17, 22, and 23). Chemical sensors were installed in Holes#20 and #21, but the sensors did not respond to the moisture in the rock. Water was collected from Zone 4 in Hole#16. Calculated temperature distribution and the measured ones will be compared in Section 4.3.1. The humidity and gas pressure measurements in Holes 16 and 18 will be discussed in Section 4.3.2. The moisture content measured by neutron logging and ERT will be presented and discussed in Sections 4.3.3 and 4.3.4. Calculated saturation distributions are presented and compared with the neutron logging results and the ERT in Section 4.3.5. The chemical composition of the water collected from Hole#16 is discussed in Section 4.3.6. Fracture closing and opening based on the thermomechanical measurements are summarized in Section 4.3.7. Air permeability changes measured in Holes #16 and #18 are presented in Section 4.3.8. An integrated discussion is presented in Section 4.3.9.

4.3.1 Temperature

Three-dimensional model calculations were conducted using NUFT code to predict the temperature and saturation distributions in the SHT. The thermal conductivities used in the calculations were 2.0 w/m-°C for saturated rock and 1.67 w/m-°C for dry rock. The permeability for the effective continuum model was assumed to be 3.3×10^{-15} m^2. The percolation flux in the model was 0.21 mm/yr. Figures 4.3.1.1 and 4.3.1.2 show the calculated temperature distributions in a vertical cross section plane through the mid-point of the heater, on May 28 (before the heater was turned off) and June 27 (one month after the heater was turned off), 1997. Figure 4.3.1.1 shows that the calculations predict that the 100°C isotherm at the end of the heating phase is about 1 m from the heater. And in the first month of cooling the temperature in the heated rock mass will decrease to about 65°C.

The measured temperatures are used to create the thermal field in a cross section area perpendicular to the mid-point of the heater on 5/22/97, 6/9/97, and 6/26/97 as shown in Figure 4.3.1.3. The 100°C isotherm was about 0.9 m from the heater. This is consistent with the temperature measured by the

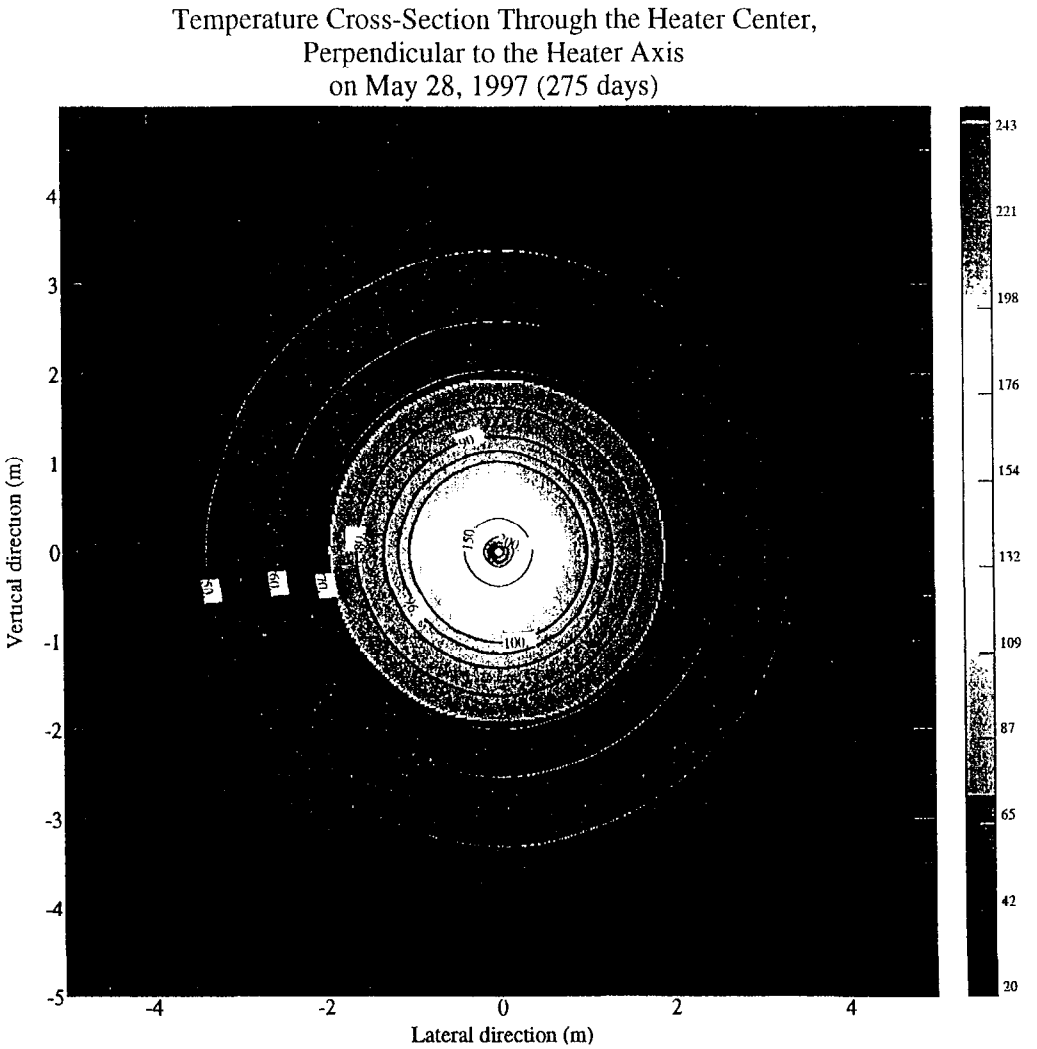

Figure 4.3.1.1. Calculated temperature distribution in a vertical cross section plane through the mid-point of the heater, on 5/28/97.

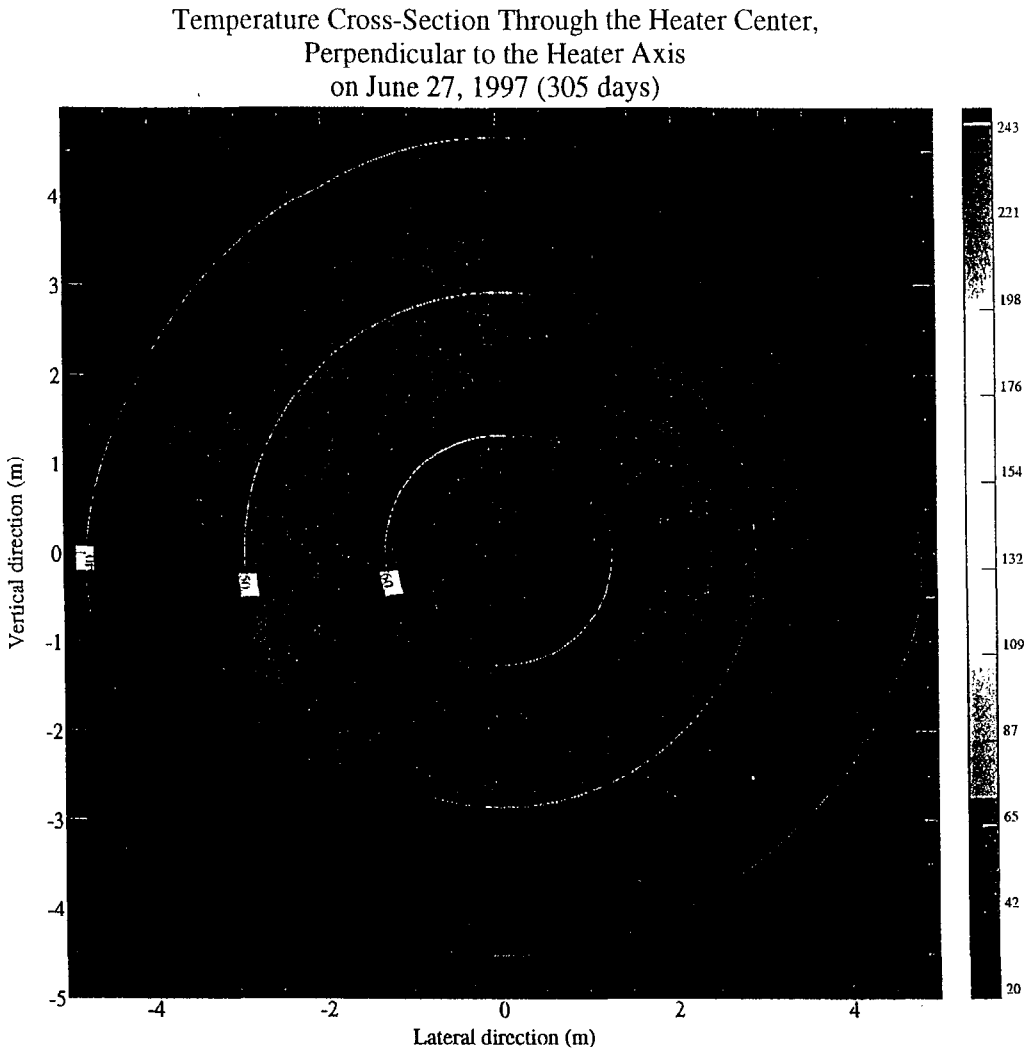

Figure 4.3.1.2. Calculated temperature distribution in a vertical cross section plane through the mid-point of the heater, on 6/27/97.

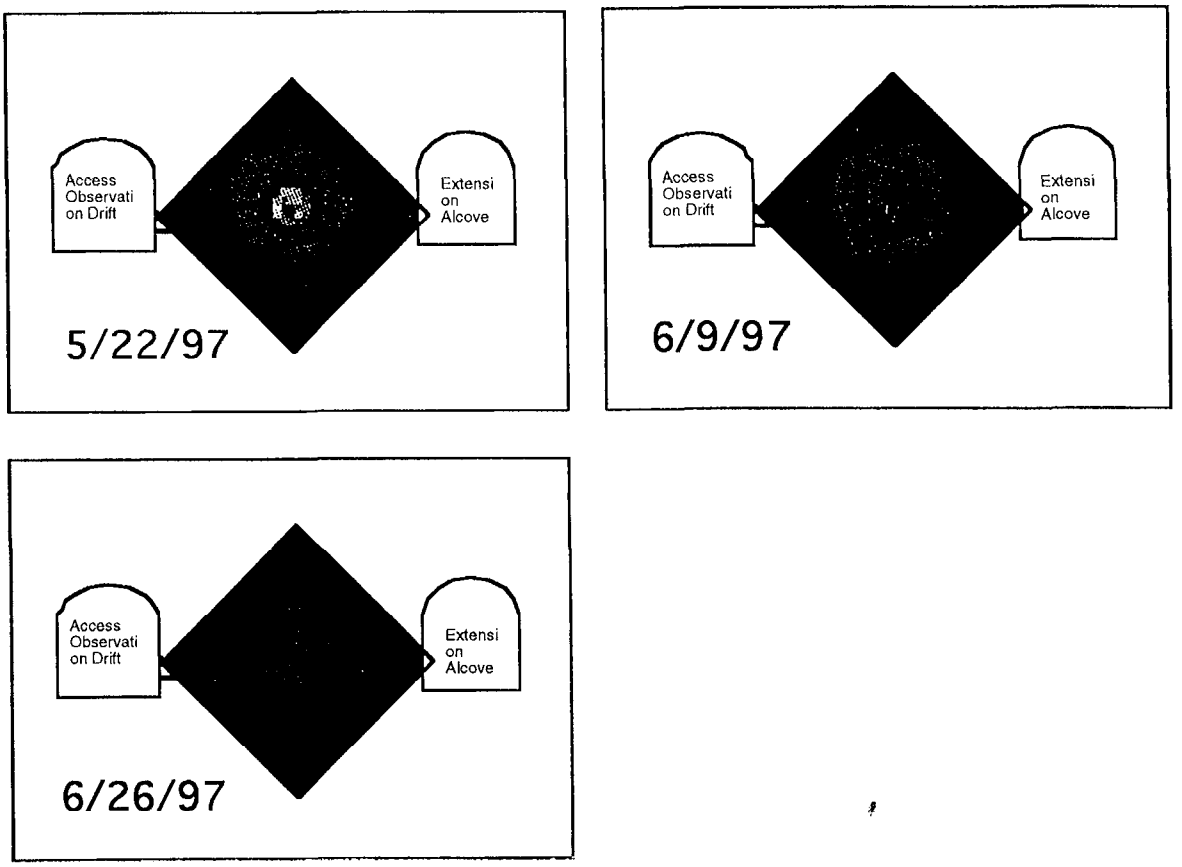

Figure 4.3.1.3. Temperature distribution in ERT plane from interpolated/extrapolated RTD and thermocouple measurements.

RTDs in Hole#17. The closest point between Hole#17 and the heater is about 1.2 m, and the peak temperature measured in that hole was 90°C. The model calculations slightly over-predicted the temperatures in the SHT, but not significant.

The peak temperatures measured in the neutron/RTD holes are 62, 90, 74, and 88°C in Holes#15, 17, 22, and 23 respectively. The shortest distance between the heater and those holes are 2.07, 1.2, 1.6, and 1.23 m respectively.

4.3.2 Humidity and Gas Pressure

Relative humidity is measured by Humicaps in four zones in each of Holes 16 and 18. Due to the limitation of the borehole size, only four packers were installed in each hole. The four zones in these holes are isolated by the inflated high temperature packers. Due to a highly fractured zone near the collar of those holes, we decided to install the packer system near the collar in order to seal those fracture zones. Zone 1 in those holes is near the collar; Zone 4 is closest to the bottom of the holes. Zones 1 to 3 are about 6.35 cm in length; the length of Zone 4 is about 2.13 m, and 1.72 m in Holes 16 and 18 respectively. The measured relative humidity as a function of time of test in those two holes are shown in Figures 4.3.2.1 to 4.3.2.2. There is no calculated relative humidity to be compared with the measured data. Figure 4.3.2.1 shows the relative humidity in Zone 3 and Zone 4 of Hole#16. The relative humidity in Zones 3 and 4 of Hole#18 are shown in Figure 4.3.2.2. The relative humidity in Zones 1 and 2 in these two holes is similar to that in Zone 3. The relative humidity in Zone 3 of Hole#16 decreased from about 92%, when the heater was energized, to about 87 % at about 1500 hour in the heating phase, then increased since. The two discontinuities between hours 2000 and 4000 were related to the sampling of water in Zone 4 of this hole. The cause of the disturbance at hour 5200 is still under investigation. The disturbance may be related to the increase of the inflation pressure in the packers conducted by Lawrence Berkeley National Laboratory (LBNL). The variation of the relative humidity in Zone 3 of Hole#18 seems not related to the activities in Hole#16. When the heater was turned off, the relative humidity in Zone 3 of both Hole#16 and Hole#18 increased. However, the relative humidity in Zone 3 of Hole#16 increased more than that in Hole#18. In Zone 4 of both holes the humidity decreased for a short period after the energization of the heater, then increased quickly to 100%. The Humicap in Zone 4 of Hole 16 ceased functioning on 11/14/96 (about 1800 hour of heating). That may be due to the flooding of that zone by the water in the hole. Base on the laboratory measurements conducted by Lin and Roberts [1], less than 50% water saturation is needed in order to generate a 100% relative humidity; the high humidity in Zone 4 is what we would expected. The lower humidity reading in the other zones indicate that there are hydrological communication between those zones and the alcoves, most likely through the fractures.

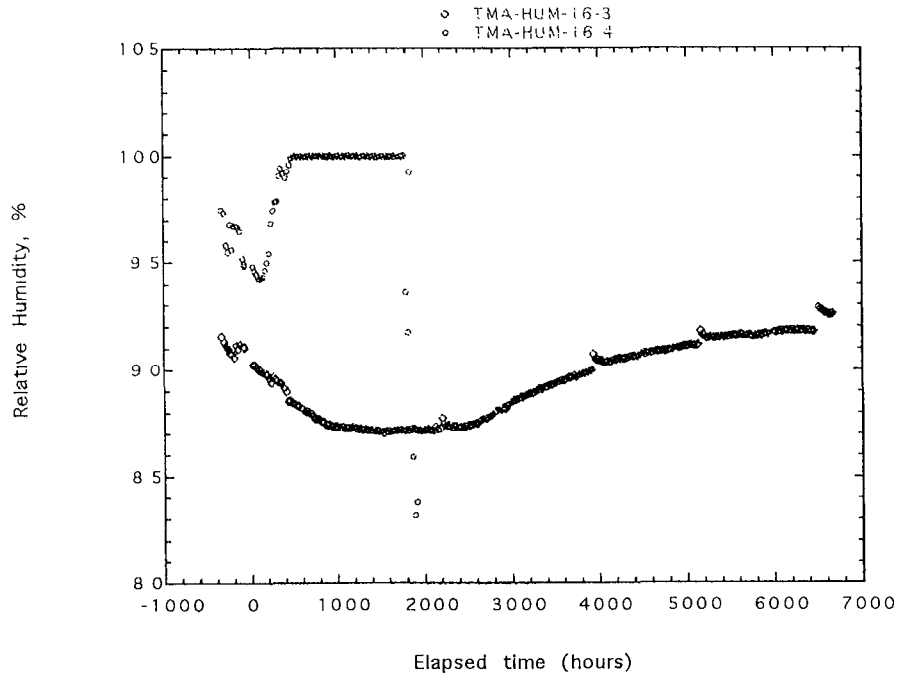

Figure 4.3.2.1. Relative humidity in Zones 3 and 4 of Hole#16 as a function of time. The 0 hour is when the heater was turned on.

Gas pressure in the same four zones in Holes 16 and 18 are measured by gauge gas pressure transducers. The transducers have an accuracy of better than 0.15% of the maximum rated pressure, which is 50 psig. Therefore the accuracy of the measured pressure shoud be better than ±0.075 psig. Figures 4.3.2.3 and 4.3.2.4 show the gas pressures in Zones 1 to 4 of Holes 16 and 18 respectively. Zone 1 is near the collar, and Zone 4 is at the bottom of the hole. The gas pressure in Zones 1, 3, and 4 of Hole#16 have been negative (less than the atmospheric pressure in the tunnel) throughout the test so far. On the other hand, the pressure in Zone 2 was positive. And the pressure in Zone 4 decreased with time, and showed episodic increases, which were probably assoicated with the withdraw of condensed water in this zone. The decreasing of pressure with time in Zone 4 of Hole#16 was probably caused by the condensation of vapor into water. There is no obvious explanation for the positive pressure in Zone 2 of Hole#16. In Hole #18, however, the pressures show a little more systematic: the pressure in Zones 1 to 3 is negative; the pressure in Zone 4 is positive. As mentioned above, Zone 4 is the only one in this hole that the relative humidity reached 100%. These phenomena in Hole 18 may be due to the flow of vapor into Zone 4, and creates draw-down in other zones.

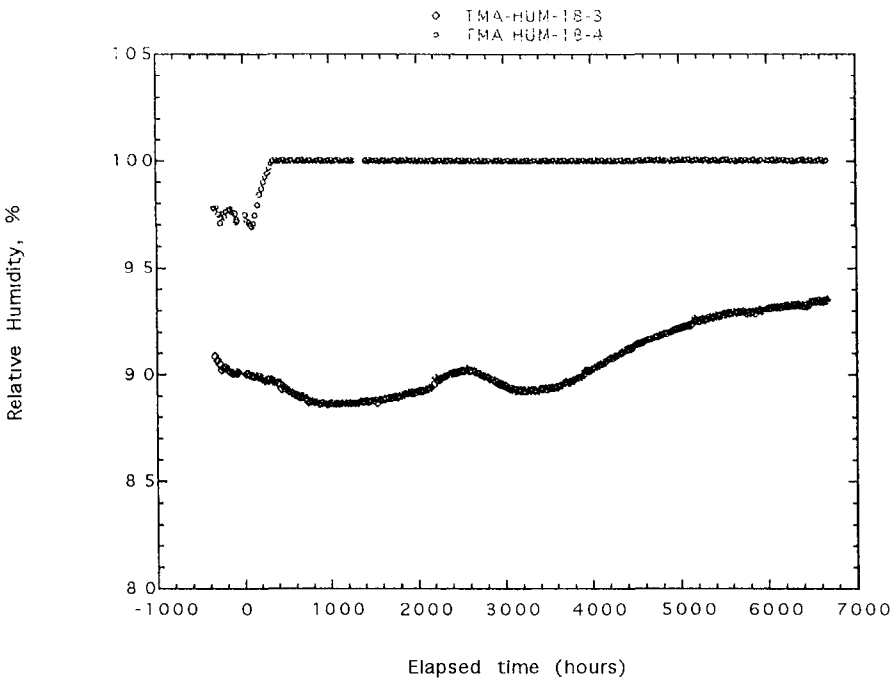

Figure 4.3.2.2. Relative humidity in Zones 3 and 4 of Hole#18 as a function of time. The 0 hour is when the heater was turned on.

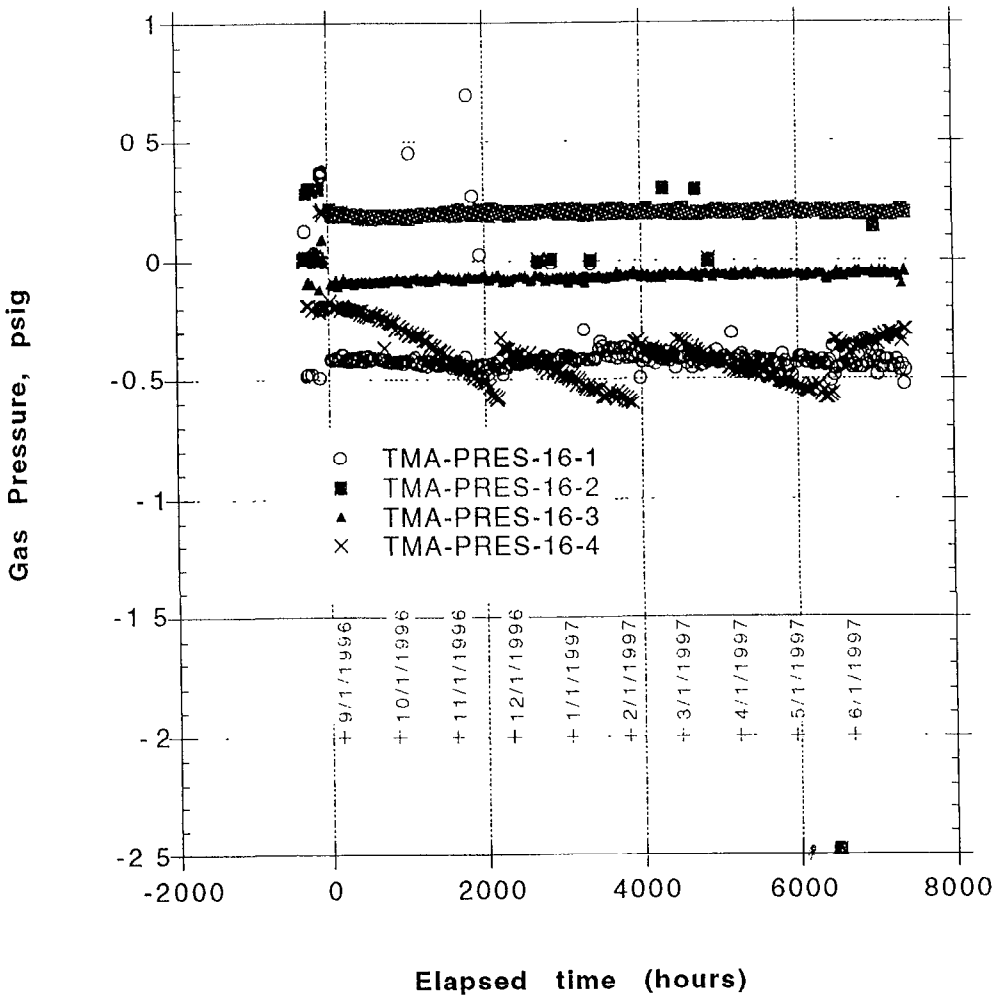

Figure 4.3.2.3. Gas pressure in four zones (16-1 to 16-4) of Hole#16 as a function of time. The 0 hour is when the heater was turned on.

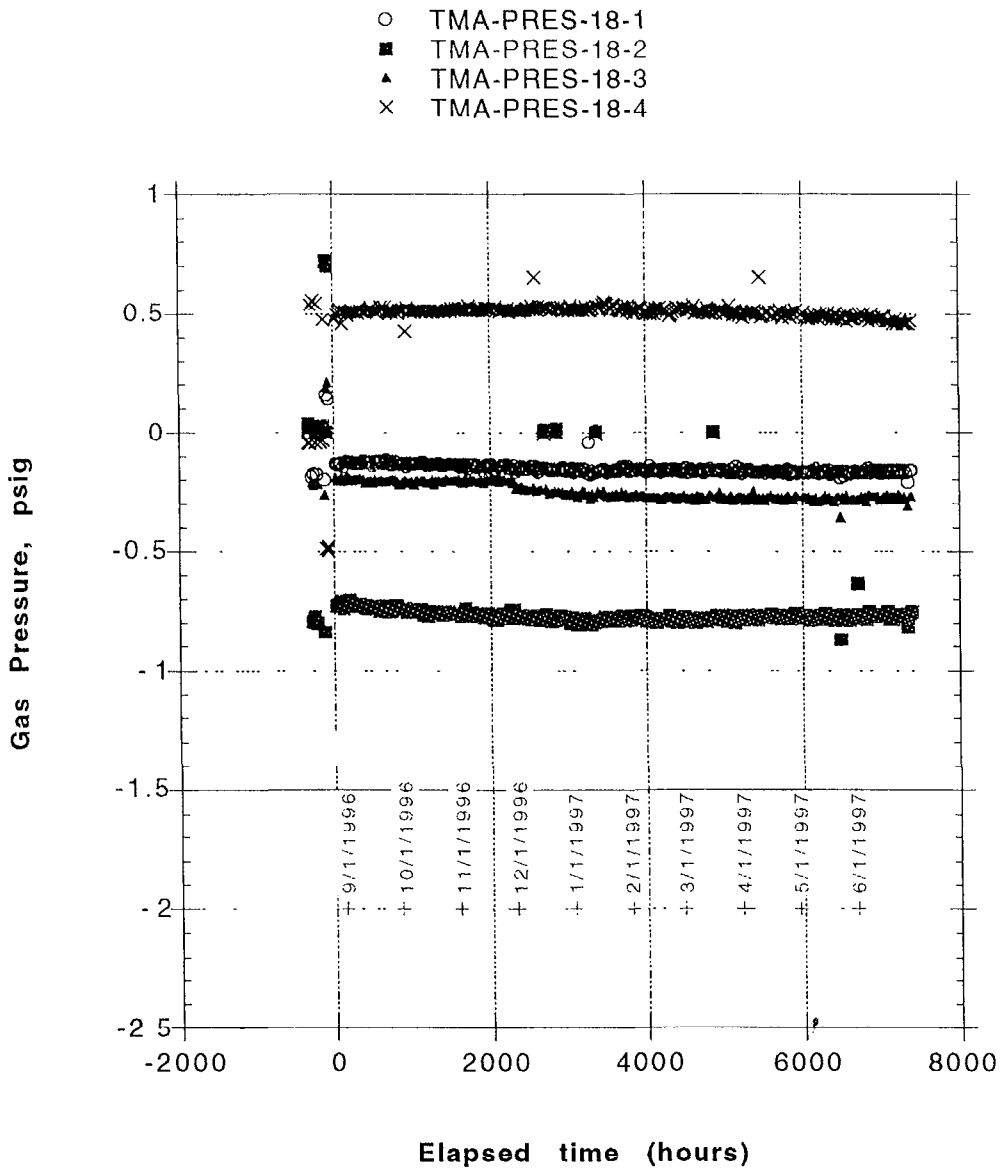

Figure 4.3.2.4. Gas pressure in four zones (18-1 to 18-4) of Hole#18 as a function of time. The 0 hour is when the heater was turned on.

4.3.3 Neutron Logging

Some of the results of the neutron logging are included in this report. A complete discussion of the neutron logging results is included in the third quarterly report of the neutron logging in the SHT (Lin and Carlson, 1997). In this report only the neutron results on 4/30/97, 5/21/97, 6/10/97, and 6/24/97 will be reported. All of the results are the difference in fraction volume water content between the in-heat and cool-down phase measurements and the pre-heat data in each hole. Therefore, a zero difference fraction volume water means no change in the moisture content; a positive difference fraction volume water content means increasing in moisture content. All of the figures shown below have the same scale in the water content so that the changes in the water contents can be compared.

Figures 4.3.3.1 and 4.3.3.2 show the neutron results in Hole#15. A drying region is seen near the closest point between the heater and this hole (about 5.75 m from the collar). The maximum decrease in the fraction volume water content in this hole was about 0.006. If we assume that the porosity of the rock mass is 0.14, as reported by the Characterization of the ESF Thermal Test Area (OCRWM M&O, 1996) for some rock samples, the fraction volume water equals a decrease in saturation level of about 4%. On the other hand, if we assume a porosity of 0.1, as reported for some other samples in the same report (OCRWM M&O, 1996), then the decrease in the saturation level will be about 6%. In any event the drying was not very significant. This is expected, because the peak temperature in this hole was only about 62°C. There is also a drying

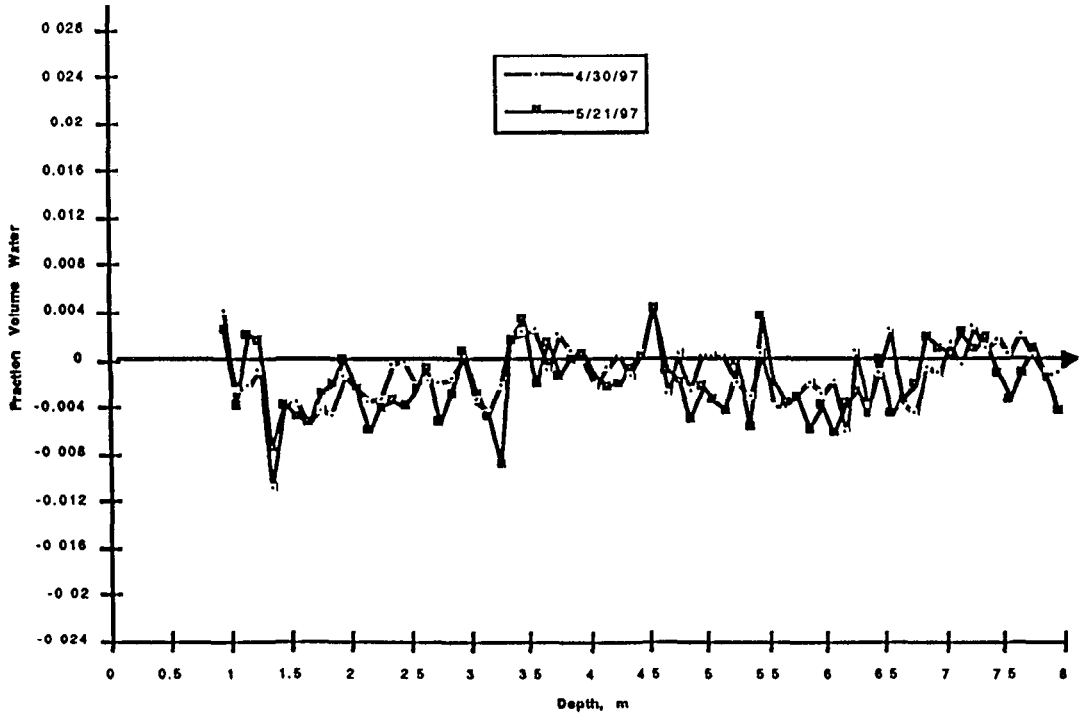

Figure 4.3.3.1. Difference fraction volume water content in Hole#15 as a function of depth from collar on 4/30/97 and 5/21/97.

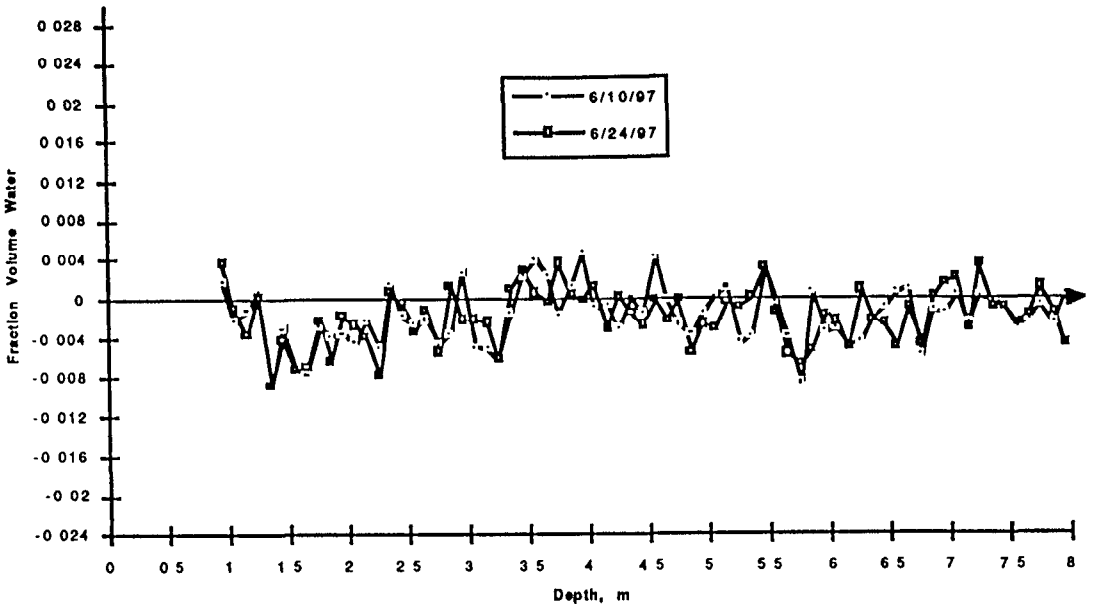

Figure 4.3.3.2. Difference fraction volume water content in Hole#15 as a function of depth from collar on 6/10/97 and 6/24/97.

region near the collar (about 1.5-m depth) of the hole. The cause of that drying is not clear yet. Figure 4.3.3.2 shows that during the first month of cooling there has been no change in the moisture content in this hole. The peak temperature in this hole has decreased to about 51°C. Apparently cooling the rock mass has not caused re-wetting in this hole.

The neutron logging results in Hole#17 at the end of the heating phase and the beginning of the cool-down phase are shown in Figures 4.3.3.3 and 4.3.3.4. A drying region is observed in this hole, centered at about the closest point between this hole and the heater (about 6.48-m depth). The maximum decrease in the fraction volume water content is about 0.014. For a porosity of 0.14, this decrease in the fraction volume water content equals to a decrease in the saturation level of about 10%; for a porosity of 0.1, the decrease in the saturation level will be about 14%. The width of this drying region is about 3 m, which is greater than that in any other holes. The peak temperature in this hole during the heating phase was about 90°C. An increase in the water content was also observed near the collar of this hole (at about 1.5-m depth). This may be caused by the shedding of water around the heater. Figure 4.3.3.4 shows the difference fraction volume water content in this hole during the first month of cooling. No change in the water content is observed in this hole during the first month of cooling. The peak temperature in this hole has decreased to about 56°C by 6/30/97. Again, as in Hole#15, the cooling has not caused re-wetting yet.

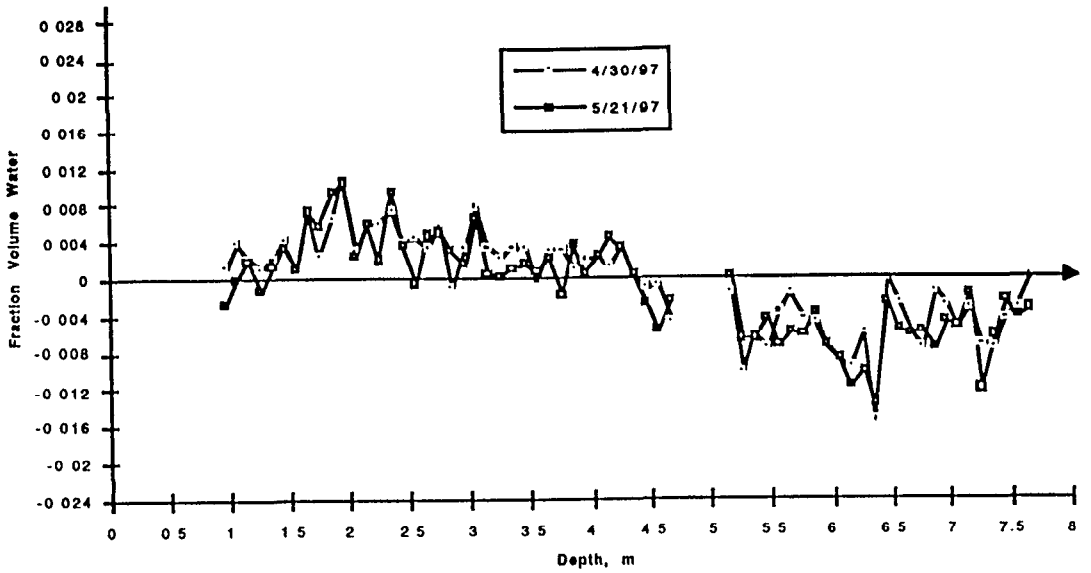

Figure 4.3.3.3. Difference fraction volume water content in Hole#17 as a function of depth from collar on 4/30/97 and 5/21/97.

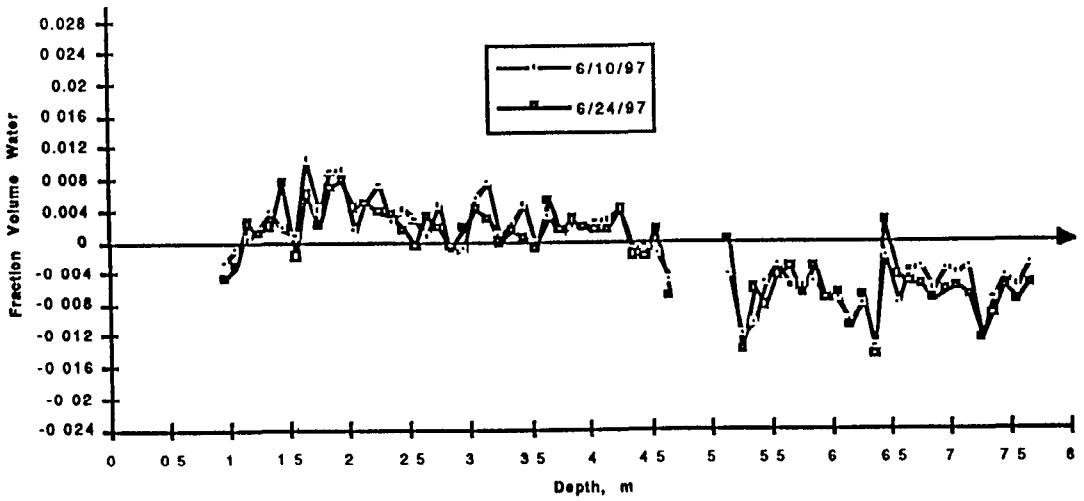

Figure 4.3.3.4. Difference fraction volume water content in Hole#17 as a function of depth from collar on 6/10/97 and 6/24/97.

Figures 4.3.3.5 and 4.3.3.6 show the neutron logging results in Hole#22 as a function of depth from collar on various dates during the heating and cool-down phases. As shown in Figure 4.3.3.5, a slight drying region near the bottom of this hole was observed at the end of the heating phase. The maximum decrease in the fraction volume water content in that region was about 0.008, slightly greater than that in Hole#15. The decrease in the sturation level is 6% and 8% for a porosity of 0.14 and 0.1 respectively. The peak temperature in this hole during the heating phase was about 74°C. As shown in

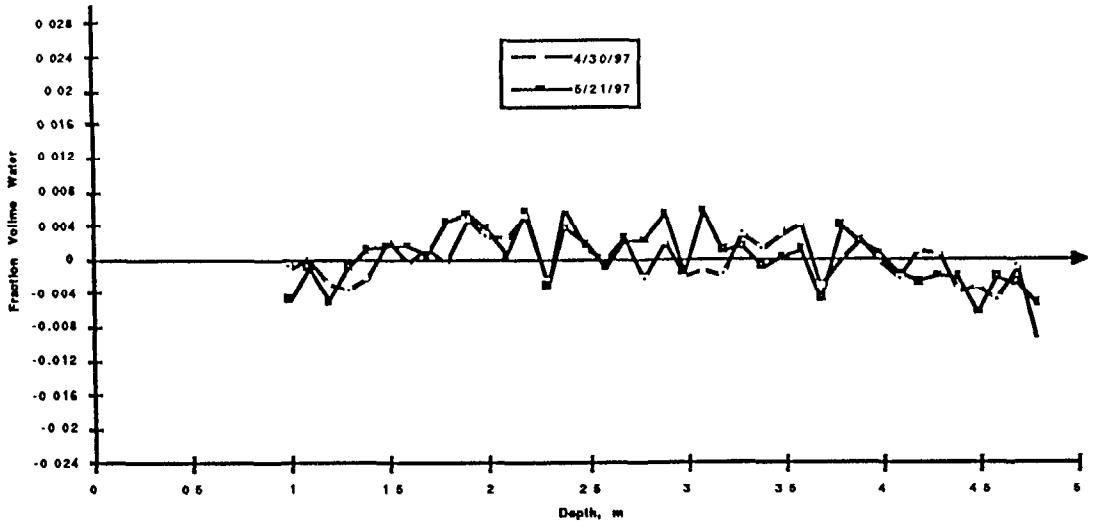

Figure 4.3.3.5. Difference fraction volume water content in Hole#22 as a function of depth from collar on 4/30/97 and 5/21/97.

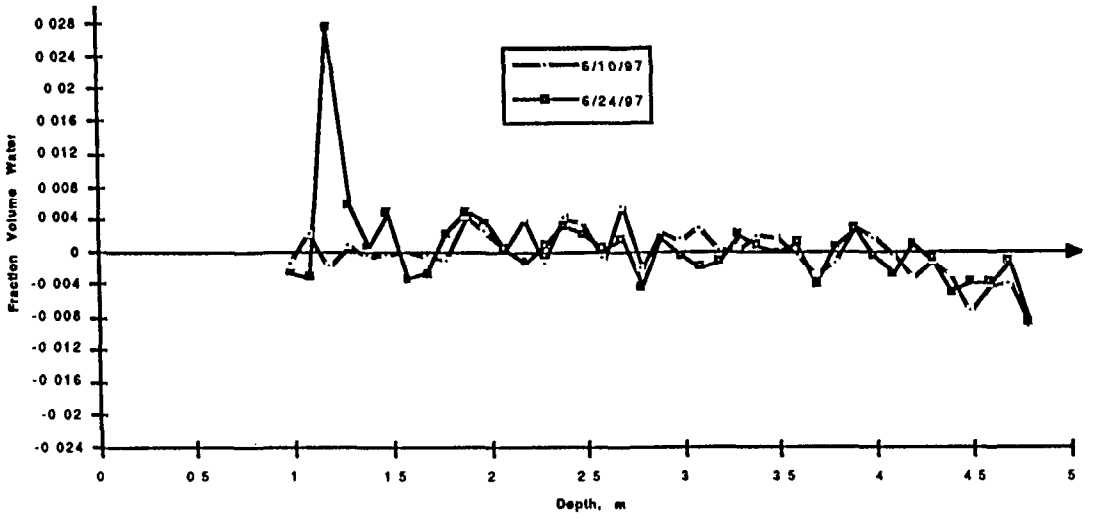

Figure 4.3.3.6. Difference fraction volume water content in Hole#22 as a function of depth from collar on 6/10/97 and 6/24/97.

Figure 4.3.3.6, the fraction volume water content in the drying region did not change during the first month of cooling. By June 30, 1997 the peak temperature in this hole has decreased to about 53°C. Again, as in Holes#15 and 17, the cooling has not caused re-wetting in this hole yet.

The difference fraction volume water content in Hole#23 as a function of depth from collar on various dates during the heating and cooling phases are shown in Figures 4.3.3.7 and 4.3.3.8. As shown in Figure 4.3.3.7, a drying region near the bottom of this hole was observed. This region was developed about two months into the heating phase. The maximum decrease in the fraction volume water content in this region was about 0.016. The decrease in water saturation was about 11% and 16% for porosities of 0.14 and 0.1 respectively. The peak temperature in this hole was about 88°C. The amplitude of the drying in this hole was slightly greater than that in Hole#17, even though the peak temperature was slightly less. This may have been affected by the orientation of the hole and the heterogeneity of the rock mass. Hole#23 reaches the upper-left side of the heated block with an inclination angle of about 7.5 degrees, while Hole#17 reaches the lower-right side of the heater with a declination angle of about 7 degrees. The width of the drying region in this hole is about 1 m, which is much less than that in Hole#17. This difference may be caused by the location of the holes relative to the heater: Hole#17 is below the heater; Hole#23 is above and to the side of the heater. As observed in the thermal test in G-Tunnel, the region below the heater tends to have a greater drying area (Ramirez, 1991). As shown in Figure 4.3.3.8, the neutron measurements on 6/10/97 and 6/24/97 show no change in the water content in this hole. The peak temperature in this hole has decreased to about 55°C by 6/30/97. Apparently, as in other holes, the cooling has not caused re-wetting in this hole yet.

In summary, the changes in water saturation in the neutron holes seem to be in consistent with the temperature measured in those holes, ie. the greater the temperature, the more decrease in saturation. Overall, the degree of drying during the heating phase was not large. Based on the neutron data, the drying (less saturation than the pre-heat background) region extended to about 2.2 m from the heater. And there was no change in saturation during the first month of cooling.

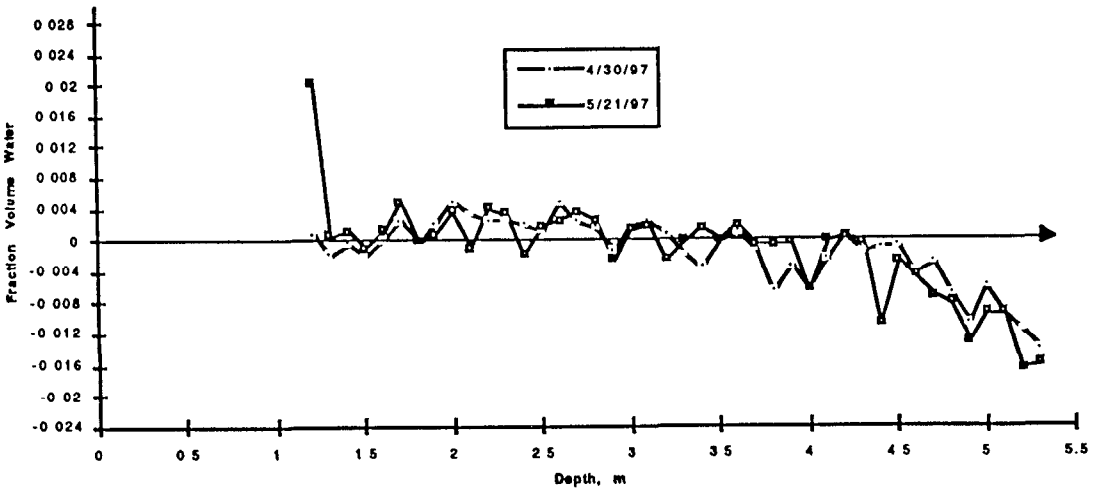

Figure 4.3.3.7. Difference fraction volume water content in Hole#23 as a function of depth from collar on 4/30/97 and 5/21/97.

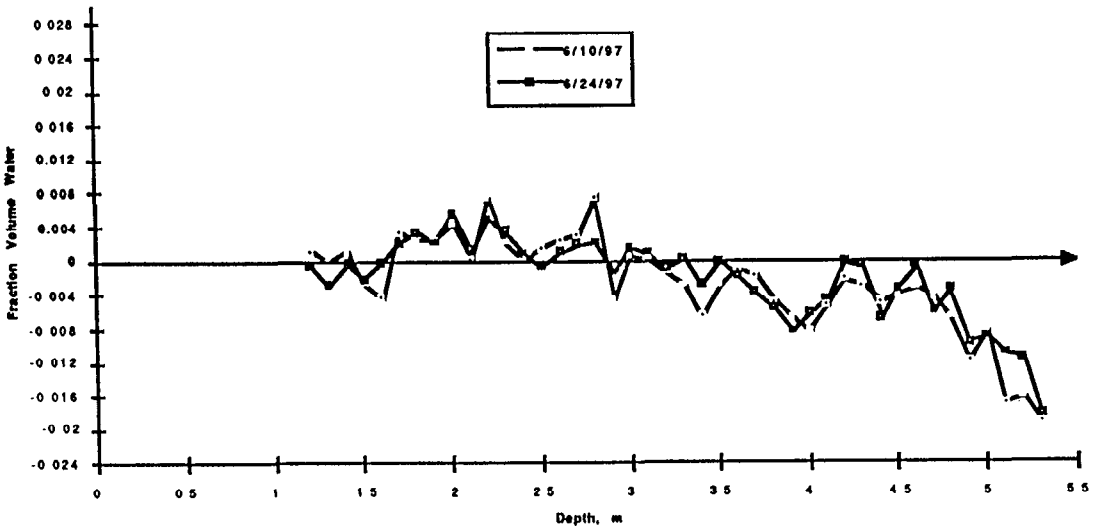

Figure 4.3.3.8. Difference fraction volume water content in Hole#23 as a function of depth on 6/10/97 and 6/24/97.

4.3.4 Electrical Resistivity Tomography

Electrical resistivity tomography (ERT) surveys were conducted during the SHT in order to map the changes in moisture content caused by temperature changes. Of particular interest, is the formation and movement of condensate within the fractured rock mass. A summary of the ERT results in the SHT is included in here. A complete discussion of the ERT methodology, data analyses, and results for the SHT is reported by Ramirez and Daily (1997).

To calculate the changes in the rock's electrical resistivity, we compared a data set obtained after heating started and a corresponding data set obtained prior to heating. We see a region of decreasing resistivity approximately centered around the heater. The size of this region grows with time and the resistivity decreases become stronger. Data collected and processed during the first six months of heating indicate that the changes in resistivity are caused mostly by increasing temperature of the rockmass pore water although saturation changes also play a role. This pattern persists for at least 59 days of heating. To this point it is likely that our images are not dominated by drying along fractures.

The data collected and processed during the third month of the heating phase shows, we believe, that heterogeneities in the rock such as fractures are affecting the drying and wetting in the rockmass. Saturation estimates have been presented. These estimates were calculated from two models derived from the Waxman Smits equation. Of the two models considered, we believe that the model that assumes dominant surface conductance (model 2) provides the most accurate estimates (Figure 4.3.4). The black lines in the ERT images in Figure 4.3.4 are locations of the neutron logging holes. During the heating phase, the saturation estimates show a region of drying around the heater although its shape appears to be controlled by heterogeneities in the formation (fractures). The drying region appears to propagate upwards and sideways and the rock appears to be dryer overall above the heater than below it. This distribution may be evidence for drainage of water out of the system through fractures. After heating ceased, the dry region around the heater appears to be rewetting slowly; wetter rock regions observed below the heater are slowly becoming smaller in size. The saturation estimates are considered "rough" estimates, and work is ongoing to better understand and improve these. We also plan to use the calibrated neutron probe data to determine which of our saturation models is most accurate.

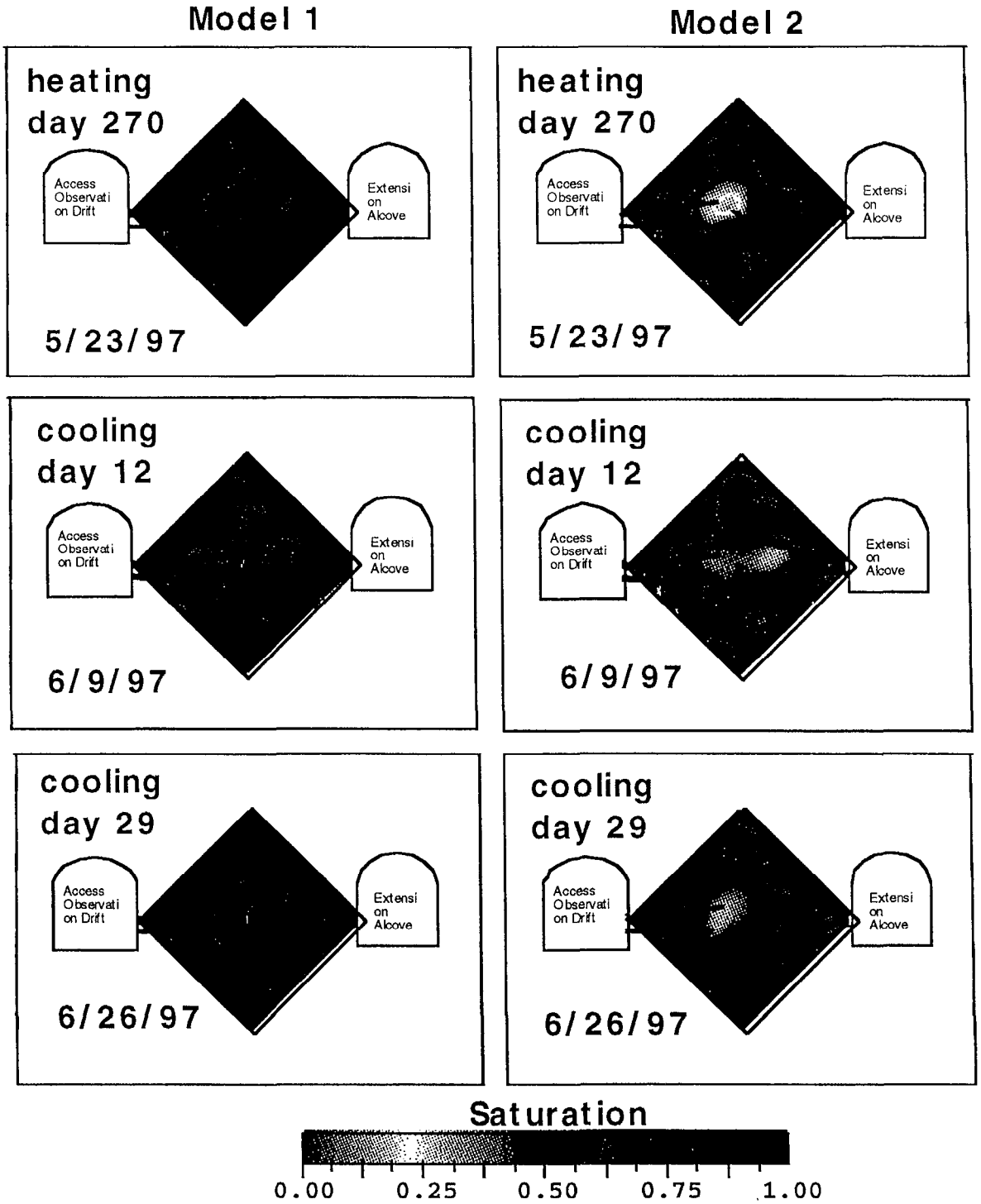

Figure 4.3.4. Estimates of saturation of the rockmass assuming the initial saturation is 0.92 and using two models (described in the text) relating moisture content to resistivity.

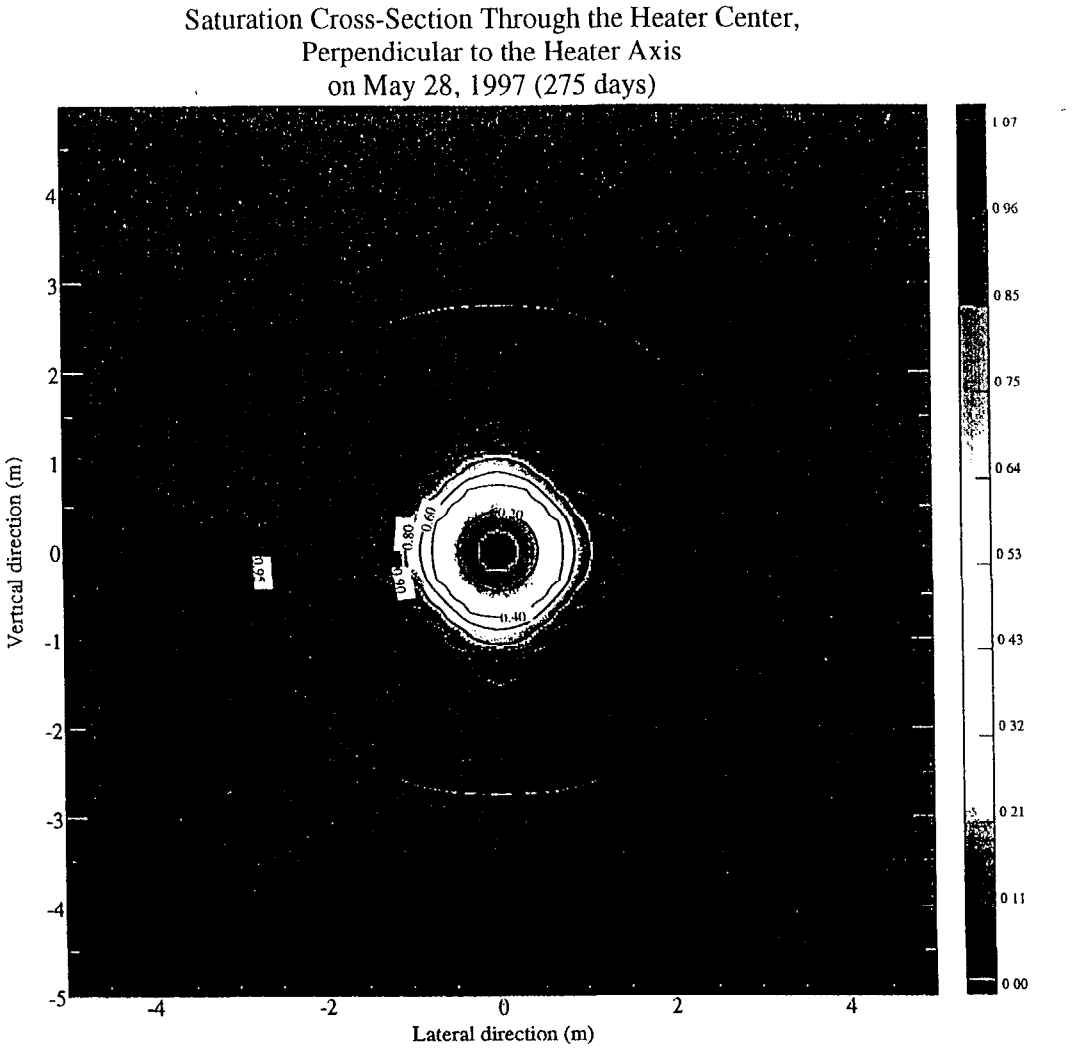

Figure 4.3.5.1. Calculated saturation distribution in a vertical cross section plane through the mid-point of the heater, on 5/28/97.

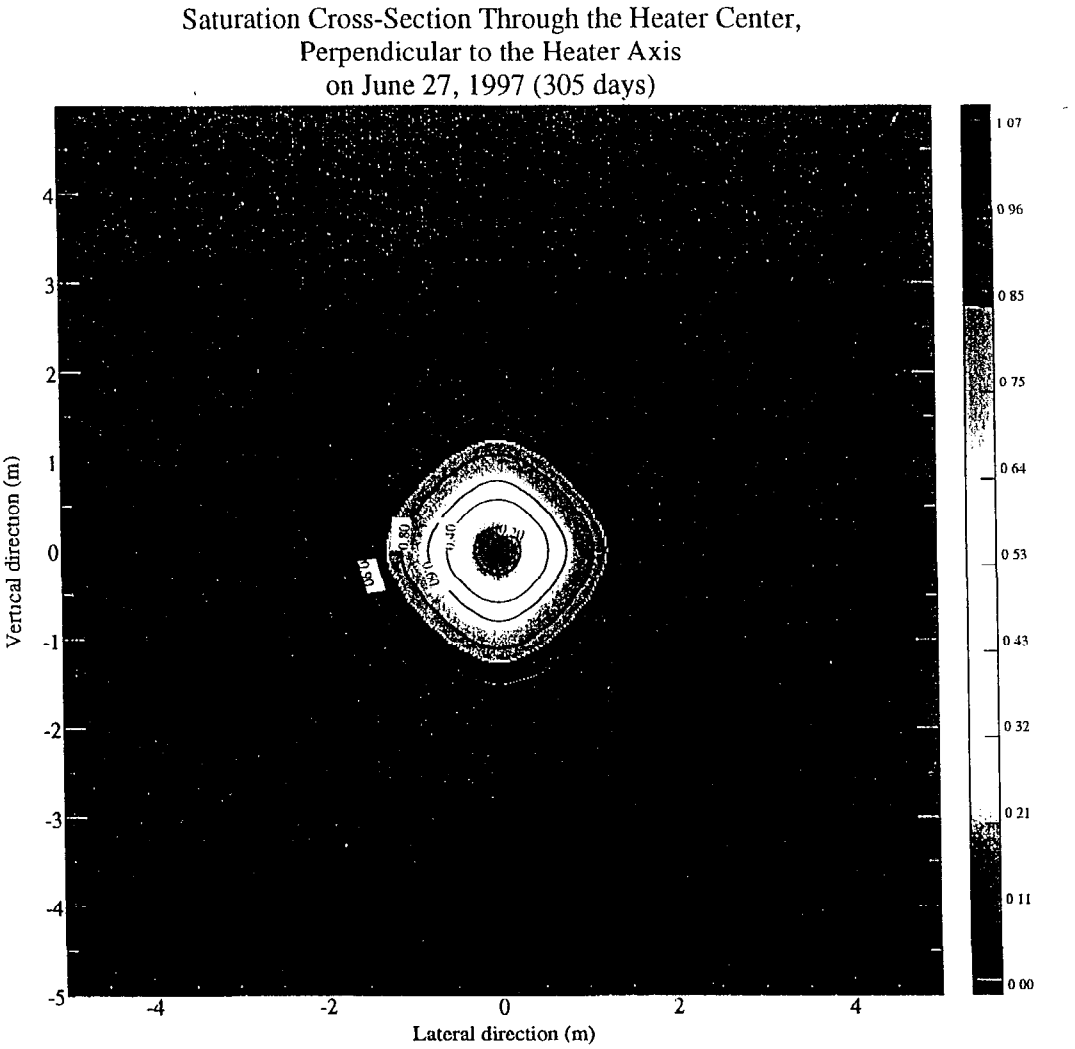

Figure 4.3.5.2. Calculated saturation distribution in a vertical cross section plane through the mid-point of the heater, on 6/27/97.

4.3.5 Model Calculations of Water Saturation

The calculated distribution of water saturation in the heated rock mass at the end of the heating phase and one month into the cooling phase are shown in Figure 4.3.5.1 and 4.3.5.2. The model predicts a drying (water saturation less than the initial level of 92%) region at the end of heating phase to be about 1.1 m from the heater, and a region of increasing saturation outside of the drying region. Within the first month of cooling the model calculations predict a re-wetting of the entire drying region, but decreasing in water saturation in the region immediately outside of the drying region during the heating phase.

The ERT measured a drying region much bigger than the predicted one, especially in regions above and to the sides of the heater. The ERT detected a wetter region during the heating phase only in the area below the heater. During the cooling phase, the ERT measured re-wetting near the center of the drying region, but not much change in saturation anywhere else.

During the heating phase, the neutron logging recorded a drying region, which is bigger than what was predicted by the model calculations, and the neutron logging did not indicate a wetter region outside of the drying region. During the first month of cooling, the neutron logging did not register any change in the saturation level.

4.3.6 Water Chemistry

As reported before, the chemical sensors installed in Holes #20 and 21 did not work in the partially saturated environment. Water was collected from Zone 4 of Hole#16, which extends from 1.23 to 3.36 m from the heater. Water was collected from that zone on three dates: 11/25/96, 2/4/97, and 2/27/97. The volume of water collected on those three dates were 5.5 l, 5.5 l, and 1.52 l respectively. The results of chemical analyses of the first two water samples, conducted by Lawrence Livermore National Laboratory (LLNL), Los Alamos National Laboratory (LANL), and US Geological Survey (USGS), are listed in Table 1. The chemistry of the water is compared with that of J-13 water, groundwater from Hole G-4, and groundwater from Rainier Mesa, which are shown in Table 2. Both water samples from Hole#16 are more dilute than J-13 water, G-4 water, and Rainier Mesa water. The only exception is the concentration of Ca. The water from Hole#16 has about the same Ca concentration as the local groundwater. This indicates that the water in Hole#16 was condensed from vapor that was moved away from the heated region by the heat. The vapor and/or the condensed water flowed along fractures into Zone 4 of Hole#16. During the flow process the vapor/water reacted with the fracture coating Ca-minerals.

Table 1. Chemical composition of the water samples from Hole#16, as analyzed by LLNL, LANL, and USGS.

	SHT Hole 16 LLNL Data	log molality LLNL Data	SHT Hole 16 LANL Data	SHT Hole 16 LLNL Data 2nd suite (SPC00521103)	USGS Analyses
Na (mg/l)	16	-3.16E+01		13.9	
Si (mg/l)	16.8	-3.22E+01		17.4	
Ca (mg/l)	13	-3.49E+01		9.76	
K (mg/l)	2.5	-4.19E+01		2.5	
Mg (mg/l)	1.63	-4.17E+01		1.16	
pH	6.2			6.9	
HCO3 (mg/l)#	188	-2.51E+01			
F (mg/l)	0.44	-4.64E+01		0.12	
Cl (mg/l)	2.54	-4.14E+01	2.1	1.45	
S (mg/l)	0.71	-4.65E+01			
SO4 (mg/l)	1.83	-4.72E+01	1.5	0.42	
PO4-3 (mg/l)	<0.03			<0.4	
Nitrite (mg/l)	<0.01			0.15	
NO3- (mg/l)	1.1	-4.75E+01		<0.4	
Li (mg/l)	<0.03			<0.03	
B (mg/l)	0.37	-4.47E+01		0.74	
Al (mg/l)	<0.06			<0.06	
Fe (mg/l)	0.74	-4.88E+01		0.13	
Sr (mg/l)	0.2	-5.64E+01		0.14	0.22
Br (mg/l)	<0.02		0.008	<0.4	
del D	-98.2				
del 18O	-13				
Tritium	0.44 + 0.19 TU				
87Sr/86Sr					0.7124

From charge balance

Table 2. Chemical composition of local groundwater near Yucca Mountain, NV.

	J-13* Harrar et al., 1990	G-4* Harrar et al., 1990	Rainier Mesa* Fracture Water Harrar et al., 1990
Na (mg/l)	45.8	57	35
Si (mg/l)	28.5	21	25
Ca (mg/l)	13	13	8.4
K (mg/l)	5	2.1	4.7
Mg (mg/l)	2.01	0.2	1.5
pH	7.4	7.7	7.5
HCO3 (mg/l)#	129	139	98
F (mg/l)	2.18	2.5	0.25
Cl (mg/l)	7.1	5.9	8.5
S (mg/l)			
SO4 (mg/l)	18.4	19	15
PO4-3 (mg/l)	<10		
Nitrite (mg/l)			
NO3- (mg/l)	8.8		
Li (mg/l)	0.048	0.067	
B (mg/l)	0.134		
Al (mg/l)	0.02		
Fe (mg/l)			
Sr (mg/l)	0.04		
Br (mg/l)			
del D	-98	-103	
del 18O	-13	-13.8	
Tritium			
87Sr/86Sr			

*From Harrar et al., 1990

4.3.7 Thermal-mechanical Observations

The following summary about possible frature closing and opening in the rock mass is extracted from the thermal-mechanical measurements reported by Sandia National Laboratories (1997). Displacement was measured by multiple point borehole extensometer (MPBX) along boreholes. Fracture closing and opening are inferred from the displacement measurements in the following MPBX holes: BX1, BX2, BX3, and BX4. BX1, 2, and 3 are parallel to the heater at distances about 0.3, 0.6 and 1.2 m from the heater respectively; BX4 is perpendicular to the heater at about 1. 5 m from the front (alcove) end of the heater. Both BX1 and BX3 are on the right-hand side (closer to the Thermomechanical Alcove Extension) of the heater; BX2 is on the left side of the heater.

Fracture closing may have occurred in the following regions: along BX1 in the inner half of the heater; along BX2 at the middle of the heater; along BX3 at the far end of the heater; and along BX3 at the middle of the heater. Fracture opening may have occurred in the following regions: along BX1 near the front end of the heater; along BX1 near the far end of the heater (after 50 days of heating); along BX2 at the far end of the heater; along BX4 about 1.2 to 2.2 m from the heater; and along BX4 about 0.2 to 1.2 m from the heater (after 100 days of heating).

4.3.8 Permeability Changes

Lawrence Berkeley National Laboratory (LBNL) conducted air permeability measurements in various zones in Hole#16 and #18 during the test. Their results are summarized in the following table.

Zone	Pre-heat Permeability	2/4/97 Permeability
16-4	1.10×10^{-14} m^2	2.58×10^{-15} m^2
18-4	1.73×10^{-13} m^2	7.93×10^{-14} m^2
16-2&4	5.27×10^{-15} m^2	2.83×10^{-15} m^2
others	no change	

The causes of the permeability decrease in Zone 4 in Hole#16 and #18 may include fracture closing, increasing in water saturation, and rock-water interaction in fractures. Zone 4 in Hole#16 and #18 are about 1.2 to 3.3 m from the heater. The thermomechanical measurements in this region did not indicate fracture closing.

4.3.9 Integrated Discussion

All of the thermal-hydrological-chemical measurement techniques (neutron logging, ERT, chemistry of water sampled, and temperature) and the thermal-hydrological model calculations agree that a drying region near the heater was created by the heating, and the moisture in the drying region has been moved away by the heating. The moisture was probably transported in vapor form, which was condensed into liquid water in a region about 2 to 3 m from the heater. Fractures are the preferred flow paths for the vapor and the condensed water. Rock-water interactions have occurred at least on the fracture surfaces. However, there are some discrepancies between the ERT and the neutron logging results. ERT shows a greater amplitude of drying than the neutron logging results. This may be due to the fact that neutron logging measures localized change in moisture content along a hole, whereas ERT monitors the moisture distribution in an entire imaging plane. The neutron logging results are in good agreement with the temperature measurement in the same holes. Both the model calculations and the ERT indicate some re-wetting after the heater was turned off. But the neutron logging did not measure any change in water saturation between the heating and the cooling phases.

The coupling between the thermal-hydrological processes and the thermal-mechanical responses of the rock mass is not conclusive. Displacement measured by the MPBX indicated that fractures in some regions may have been closing, while others may have been opening.

The decrease in gas permeability in Zone 4 of both Hole#16 and #18, as measured by LBNL, may be caused by fracture closing, and/or the increase in water saturation. It is also possible that the rock-water interaction in the fractures may have contributed to the decrease in the permeability.

References

Lin, W. and R. Carlson, 1997, *Neutron logging measurements in the Single Heater Test*, Third Quarter FY97 Results of Neutron Logging Measurements in the Single Heater Test, Milestone #SP9255M4, Lawrence Livermore National Laboratory, Livermore, CA.

Office of Civillian Radioactive Waste Management System Management & Operation Contractor, 1996, Characterization of the ESF Thermal Test Area, B00000000-01717-5705-00047 Rev01, TRW Environmental Safety System, Inc., Las Vegas, NV 89109

Ramirez, A., 1991, *Prototype Engineering Barrier System Field Tests (PEBSFT) Final Report*, Lawrence Livermore National Laboratory Report, UCRL-ID-106159, Livermore, CA .

Ramirez, A. and W. Daily, 1997, *Electrical Resistivity Monitoring of the Thermomechanical Heater Test in Yucca Mountain*, Third Quarter FY97 Results of ERT Measurements in the Single Heater Test, Milestone #SP9251M4, Lawrence Livermore National Laboratory, Livermore, CA.

Sandia National Laboratories, 1997, Evaluation of Single Heater Test Thermal and Thermomechanical Data: Second Quarter Results (8/26/96 through 2/28/97), Albuquerque, NM 87185.

Technical Information Department • **Lawrence Livermore National Laboratory**
University of California • Livermore, California 94551